

## Reversibly Switching the Surface Porosity of a DNA Tetrahedron

Chuan Zhang,<sup>†</sup> Cheng Tian,<sup>†</sup> Xiang Li,<sup>†</sup> Hang Qian,<sup>†,§</sup> Chenhui Hao,<sup>†</sup> Wen Jiang,<sup>‡</sup> and Chengde Mao<sup>\*,†</sup>

<sup>†</sup>Department of Chemistry and <sup>‡</sup>Markey Center for Structural Biology and Department of Biological Sciences, Purdue University, West Lafayette, Indiana 47907, United States

<sup>§</sup>College of Chemistry and Chemical Engineering, Xiamen University, Xiamen 361005, China

**S** Supporting Information

**ABSTRACT:** The ability to reversibly switch the surface porosity of nanocages would allow controllable matter transport in and out of the nanocages. This would be a desirable property for many technological applications, such as drug delivery. To achieve such capability, however, is challenging. Herein we report a strategy for reversibly changing the surface porosity of a self-assembled DNA nanocage (a DNA tetrahedron) that is based on DNA hybridization and strand displacement. The involved DNA nanostructures were thoroughly characterized by multiple techniques, including polyacrylamide gel electrophoresis, dynamic light scattering, atomic force microscopy, and cryogenic electron microscopy. This work may lead to the design and construction of stimuli-responsive nanocages that might find applications as smart materials.

DNA, as a programmable construction material,<sup>1–3</sup> has been used to construct a wide range of nanostructures, including various nanocages.<sup>4–24</sup> Such DNA nanocages have been demonstrated to be able to encapsulate guest objects.<sup>17–19</sup> Under certain conditions, the DNA cages can open and release the guests.<sup>19</sup> Such behavior has been proposed for controlled delivery and nanoguest organization.<sup>13</sup> In this work, we have developed a strategy to reversibly cap the surface pores of DNA framework polyhedra by a capping motif (CM). Each DNA polyhedron contains multiple pores on its surface that are related to each other by the polyhedral symmetries. The opening/closing process simultaneously takes place at all surface pores.

Figure 1 illustrates the reversible capping/uncapping process in the DNA tetrahedron (TET) surface pores. This study is based on a symmetric DNA tetrahedral nanocage structure,<sup>20</sup> and the dynamic process is based on toeholdless strand displacement. In our previous studies, star-shaped DNA nanomotifs were programmed to self-assemble into symmetric DNA polyhedra through hybridization between single-stranded overhangs (sticky ends).<sup>20–24</sup> Here we extended the single-stranded overhangs by 10 nucleotides (nt) beyond the sticky-end regions. Upon formation, the DNA TET exhibits extra single-stranded, 10 nt tails that are near the middle of the struts and point to the surface pores. Such tails provide opportunities for the tailed-TET to interact with other DNA nanostructures via single-strand hybridization. To cap the surface pores of the tailed-TET, we designed a CM consisting of a circular, threefold-repeating long strand (CL, 63 nt) and three identical copies of a short strand (CS, 14 nt). The CM contains three 7

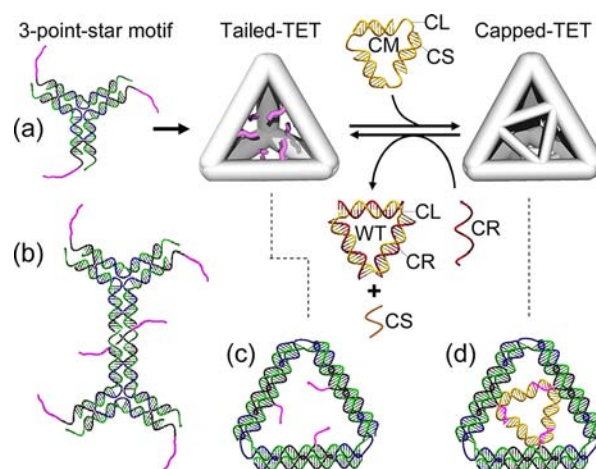


**Figure 1.** Reversible capping and uncapping of the faces of a DNA tetrahedron (TET). (a) Scheme of the overall process. Four seven-strand-containing, three-point-star motifs can self-assemble into a TET. Since each face contains three tails (purple), the TET is named tailed-TET. Each TET face can bind through base pairing to a DNA capping motif (CM) containing one circular, threefold-repeating long strand (CL) and three copies of a short strand (CS), resulting in a capped-TET. The cap can be removed by addition of a cap-removal strand (CR). Three CR strands can bind to the CL strand and displace the tails and CS strands, affording the original tailed-TET, a fully base-paired CL-3CR waste triangle (WT), and free CS strands. (b) Details of the interaction between two three-point-star motifs. (c, d) Face structures of (c) a tailed-TET and (d) a capped-TET.

nt single-stranded regions that are complementary to the seven bases at the far ends of the TET tails. When the CM is added to the tailed-TET, it binds to the tailed-TET at the surface pores and reduces the pore sizes, thus capping the tailed-TET. Furthermore, the CM can be removed from the capped-TET by addition of a 21 nt cap-removal strand (CR), which displaces CS strands and TET tails from the CL strand because a CR strand and the CL strand can form a longer [21 base pair (bp)], nick-free, continuous DNA duplex. Thus, the capped-TET is restored to uncapped tailed-TET.

The introduction of tails does not affect the self-assembly of the DNA TET from three-point-star motifs, each of which contains one long, threefold-repeating strand (L, colored blue in Figure 1), three copies of medium strands (M, green), and three copies of short, peripheral strands (S, black-and-purple).

Received: June 19, 2012

Published: July 16, 2012

The purple segment of each S strand is not involved in the TET self-assembly and remains a single-stranded tail upon TET formation. TETs with or without tails have roughly the same size and geometry; thus, they would be expected to have similar electrophoretic mobilities. The tailed-TET migrates very similarly to but slightly slower than the previous thoroughly characterized TET (Figure S1 in the Supporting Information). The polyacrylamide gel electrophoresis (PAGE) study indicated that the tailed-TET forms well. Decreasing the DNA concentration greatly reduces the formation of undesired DNA complexes with high molecular weight. When the DNA concentration is decreased to below 100 nM, the tailed-TET becomes the dominating product (>70% yield).

The capping process was first studied by native PAGE (Figure 2a). Addition of the CMs causes an obvious shift in the

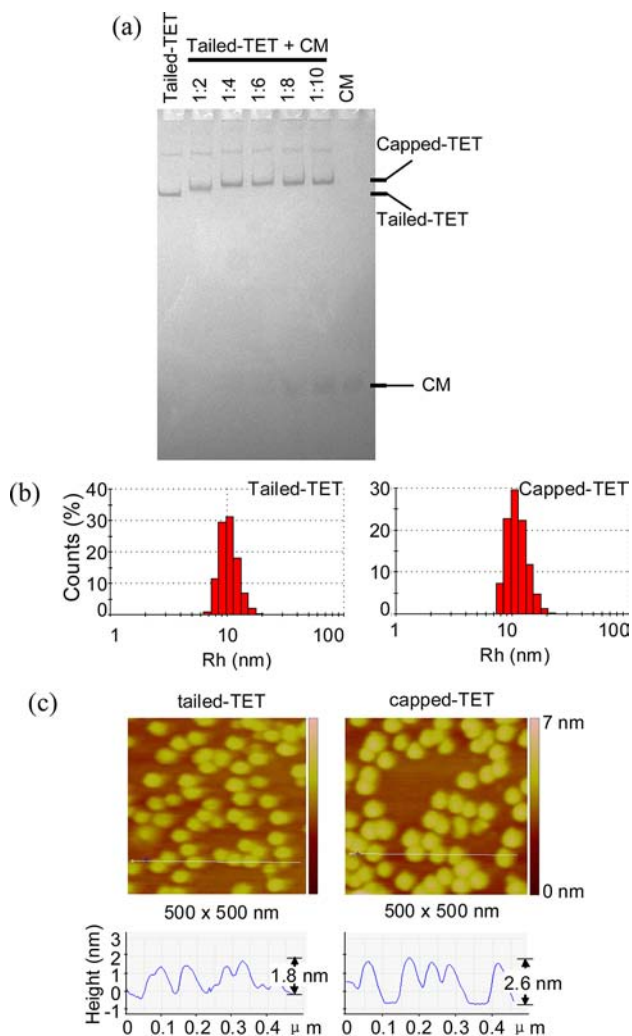


**Figure 2.** Characterization of tailed-TET and capped-TET by (a) PAGE, (b) DLS, and (c) AFM. In (c), height scale bars are shown to the right of the images, and below each AFM image is the corresponding height section analysis.

mobility for the tailed-TET because the molecular weight of the TET becomes higher upon binding of CMs. When the molar ratio between the tailed-TET and CM reaches 1:4, all four faces of TET become capped. At any ratio higher than 1:4, tailed-TET cannot bind any more CMs; thus, the mobility of the

capped-TET does not change any further, and excess CMs appear on the gel.

Capping would not be expected to change the overall physical dimensions of the TET, and this was confirmed by a dynamic light scattering (DLS) study (Figure 2b). The observed hydrodynamic radii ( $R_h$ ) are indeed similar for tailed-TET ( $10.14 \pm 0.39$  nm) and capped-TET ( $10.81 \pm 0.65$  nm). Under atomic force microscopy (AFM) imaging in air (Figure 2c and Figure S2), both tailed-TET and capped-TET appear to be well-dispersed, uniformly sized particles, consistent with the PAGE results. Because of dehydration and strong sample–substrate interactions, the absolute height values are not meaningful, but the relative height change is consistent with expectations. The tailed-TET structure contains four empty triangular faces and is quite open. It easily collapses on the mica surface and shows an average height of 1.8 nm. In contrast, the capped-TET has compact faces and collapses to a lesser extent, showing an average height of 2.6 nm.

To reveal the 3D structure of the capped-TET, we further characterized the DNA complex by cryogenic electron microscopy (cryoEM) (Figure 3). In the raw cryoEM images

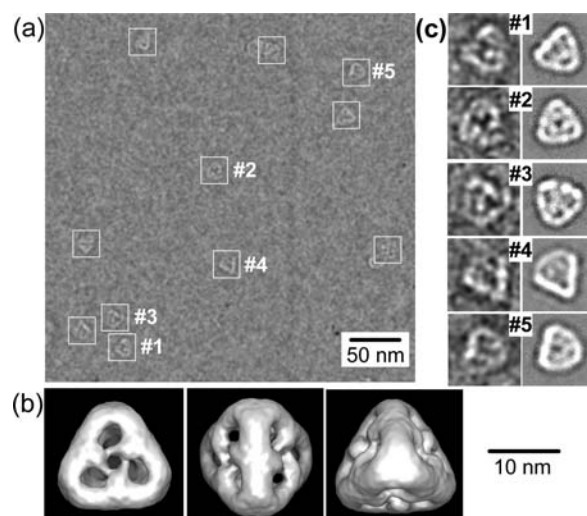


**Figure 3.** CryoEM characterization of capped-TET. (a) Raw cryoEM image of the capped-TET sample. (b) Three views of the reconstructed structural model of the capped-TET. (c) Comparison between the raw cryoEM images of individual capped-TETs and the 2D projections of the reconstructed structural model.

(Figure 3a and Figure S3), many visible particles show tetrahedral shapes with the expected size. The observed edges are  $\sim 14$  nm long, consistent with the value calculated from the designed model (13.8 nm), taking a pitch of 0.33 nm/bp and a diameter of 2 nm for a DNA duplex. With experimentally observed particles, the native structure of the DNA complex was reconstructed by single-particle 3D reconstruction,<sup>25,26</sup> a well-developed technique in structural biology that has been successfully used in structural DNA nanotechnology.<sup>13,20–24</sup> The structure was mapped to a resolution of 2.9 nm (Figure 3b) and is clearly consistent with our design. Computed 2D projections of the reconstructed structural model match very well with the images of individual raw particles (Figure 3c) and the class averages of raw particles with similar orientations (Figure S4). These results further confirm that the reconstructed model is truly the native structure of the DNA complex.

All of the above data demonstrate that the CM successfully caps each face of the TET via DNA hybridization. Furthermore, the CM can be readily removed from the capped-TET by strand displacement. When CR strands are added to the solution of capped-TETs, they bind to CL strands and displace CS strands and the TET tails, affording the original tailed-TET, a triangular waste complex (WT), and free CS strands (Figure 1). To monitor the uncapping process, we used the native PAGE technique because tailed-TET migrates faster than capped-TET in electrophoresis (Figure 4). The reversibility of the capping/uncapping process was clearly demonstrated by performing two capping/uncapping cycles.

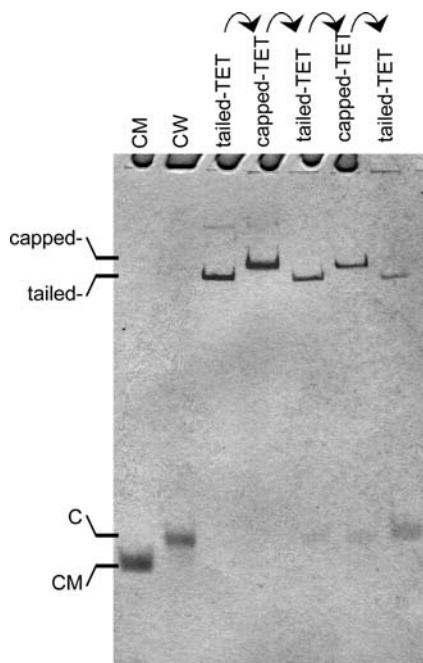


**Figure 4.** Reversible capping and uncapping of tailed-TET. The sample compositions are indicated above the gel image, and the band identities are indicated to the left of the gel. The arrows at the top indicate the capping/uncapping process.

Strand displacement is commonly initiated by a toehold on the strand to be displaced.<sup>27</sup> The process produces more base pairs and reduces the number of free bases. In this study, no toehold was used, and the mechanism is quite different. Here, none of the overall numbers of base pairs and free bases changes. The only net effect is that two short helical domains (with lengths of 7 and 14 bp) are replaced by a long helical domain (21 bp). In the absence of CR strands, the CM stably binds to the tailed TET through a trivalent interaction. Each interaction is a 7 bp hybridization. Under our experimental conditions (37 °C), such short duplexes are highly dynamic and have a high level of breathing. Stochastically, CL strands dissociate from TET tails and bind to CR strands. Branch migration then leads to further displacement of the CS strands by the CR strands, resulting in a stable 21 bp continuous duplex. Thus, strong binders can displace weaker binders that are involved in collectively strong, multivalent interactions. From our experimental data, this strand displacement is quite effective. We expect that such a toehold-free mechanism will become a powerful tool in dynamic DNA nanostructures, such as DNA nanomechanical devices and biosensors.

In summary, we have developed a strategy to reversibly switch the surface pore sizes of self-assembled DNA polyhedra. It would be important for expanding the applications of nanocages in controlled drug delivery, nano-object encapsulation, and stimuli-responsive cargo release. Investigations along this line are being very actively pursued in our group.

## ■ ASSOCIATED CONTENT

### 📄 Supporting Information

Materials and methods and additional experimental data. This material is available free of charge via the Internet at <http://pubs.acs.org>.

## ■ AUTHOR INFORMATION

### Corresponding Author

mao@purdue.edu

### Notes

The authors declare no competing financial interest.

## ■ ACKNOWLEDGMENTS

We thank the Office of Naval Research for supporting this research. AFM and DLS studies were carried out at the Purdue Laboratory for Chemical Nanotechnology (PLCN). The cryoEM images were taken at the Purdue Biological Electron Microscopy Facility, and the Purdue Rosen Center for Advanced Computing (RCAC) provided the computational resources for the 3D reconstructions.

## ■ REFERENCES

- (1) Seeman, N. C. *Nature* **2003**, *421*, 427.
- (2) Seeman, N. C. *Annu. Rev. Biochem.* **2010**, *79*, 65.
- (3) Lin, C.; Liu, Y.; Yan, H. *Biochemistry* **2009**, *48*, 1663.
- (4) Chen, J. H.; Seeman, N. C. *Nature* **1991**, *350*, 631.
- (5) Zhang, Y. W.; Seeman, N. C. *J. Am. Chem. Soc.* **1994**, *116*, 1661.
- (6) Shih, W. M.; Quispe, J. D.; Joyce, G. F. *Nature* **2004**, *427*, 618.
- (7) Goodman, R. P.; Schaap, A. T.; Tardin, C. F.; Erben, C. M.; Berry, R. M.; Schmidt, C. F.; Turberfield, A. J. *Science* **2005**, *310*, 1661.
- (8) Aldaye, F. A.; Sleiman, H. F. *J. Am. Chem. Soc.* **2007**, *129*, 13376.
- (9) Andersen, F. F.; Knudsen, B.; Oliveira, C. L. P.; Fröhlich, R. F.; Krüger, D.; Bungert, J.; Agbandje-McKenna, M.; McKenna, R.; Juul, S.; Koch, J.; Rubinstein, J. L.; Guldbrandtsen, B.; Hede, M. S.; Karlsson, G.; Andersen, A. H.; Pedersen, J. S.; Knudsen, B. R. *Nucleic Acids Res.* **2008**, *36*, 1113.
- (10) Zimmermann, J.; Cebulla, M. P. J.; Mönninghoff, S.; von Kiedrowski, G. *Angew. Chem., Int. Ed.* **2008**, *47*, 3626.
- (11) Douglas, S. M.; Dietz, H.; Liedl, T.; Högberg, B.; Franziska Graf, F.; Shih, W. M. *Nature* **2009**, *459*, 414.
- (12) Kuzuya, A.; Komiyama, M. *Chem. Commun.* **2009**, 4182.
- (13) Andersen, E. S.; Dong, M.; Nielsen, M. M.; Jahn, K.; Subramani, R.; Mamdouh, W.; Golas, M. M.; Sander, B.; Stark, H.; Oliveira, C. L. P.; Pedersen, J. S.; Virkedal, V.; Besenbacher, F.; Gothelf, K. V.; Kjems, J. *Nature* **2009**, *459*, 73.
- (14) Ke, Y. G.; Sharma, J.; Liu, M. H.; Jahn, K.; Liu, Y.; Yan, H. *Nano Lett.* **2009**, *9*, 2445.
- (15) Li, Z.; Wei, B.; Nangreave, J.; Lin, C.; Liu, Y.; Mi, Y.; Yan, H. *J. Am. Chem. Soc.* **2009**, *131*, 13093.
- (16) Wong, N.; Zhang, C.; Tan, L.; Lu, Y. *Small* **2011**, *7*, 1427.
- (17) Bhatia, D.; Mehtab, S.; Krishnan, R.; Indi, S. S.; Basu, A.; Krishnan, Y. *Angew. Chem., Int. Ed.* **2009**, *48*, 4134.
- (18) Zhao, Z.; Jacovetty, E. L.; Liu, Y.; Yan, H. *Angew. Chem., Int. Ed.* **2011**, *50*, 2041.
- (19) Lo, P. K.; Karam, P.; Aldaye, F. A.; McLaughlin, C. K.; Hamblin, G. D.; Cosa, G.; Sleiman, H. F. *Nat. Chem.* **2010**, *2*, 319.
- (20) He, Y.; Ye, T.; Su, M.; Zhang, C.; Ribbe, A. E.; Jiang, W.; Mao, C. *Nature* **2008**, *452*, 198.

- (21) Zhang, C.; Su, M.; He, Y.; Zhao, X.; Fang, P.; Ribbe, A. E.; Jiang, W.; Mao, C. *Proc. Natl. Acad. Sci. U.S.A.* **2008**, *105*, 10665.
- (22) Zhang, C.; Ko, S. H.; Su, M.; Leng, Y.; Ribbe, A. E.; Jiang, W.; Mao, C. *J. Am. Chem. Soc.* **2009**, *131*, 1413.
- (23) He, Y.; Su, M.; Fang, P.; Zhang, C.; Ribbe, A. E.; Jiang, W.; Mao, C. *Angew. Chem., Int. Ed.* **2010**, *49*, 748.
- (24) Zhang, C.; Su, M.; He, Y.; Leng, Y.; Ribbe, A. E.; Wang, G.; Jiang, W.; Mao, C. *Chem. Commun.* **2010**, *46*, 6792.
- (25) Ludtke, S. J.; Baldwin, P. R.; Chiu, W. J. *Struct. Biol.* **1999**, *128*, 82.
- (26) Goddard, T. D.; Huang, C. C.; Ferrin, T. E. *J. Struct. Biol.* **2007**, *157*, 281.
- (27) Yurke, B.; Turberfield, A. J.; Mills, A. P., Jr.; Simmel, F. C.; Neumann, J. L. *Nature* **2000**, *406*, 605.